Available online at www.sciencedirect.com
ScienceDirect
Cement & Concrete Composites 30 (2008) 334–346
Cement & Concrete Composites
www.elsevier.com/locate/cemconcomp

Effect of DMA–MMA diblock copolymer on the properties of Portland and composite cement

A. Olgun [a,*], N. Atar [a], V. Bütün [b], Y. Erdogan [a]

[a] Department of Chemistry, Dumlupinar University, Kütahya, Turkey
[b] Department of Chemistry, Eskişehir Osmangazi University, Eskişehir 26040, Turkey

Received 17 March 2006; received in revised form 29 March 2007; accepted 4 May 2007
Available online 18 May 2007

Abstract

In this paper, the effect of DMA–MMA diblock copolymer on the properties of ordinary Portland cement and cement containing boron has been studied. Variation in setting time, compressive strength and volume expansion has been determined. Cement hydration was monitored by X-ray diffraction (XRD) and by Fourier transforms infrared spectroscopy, in combination with the thermoanalytical methods (TG/DTA). The microstructural observation of the hydrated cement paste was performed by scanning electron microscopy (SEM). The result showed that DMA–MMA prolongs the early setting time of the Portland cement and composite cement, and had no noticeable effect on the final setting time of the both cement types. DMA–MMA diblock copolymer reduced the water-to-cement ratios (w/c) from 0.5 to 0.42, which improved the compressive strength of the mortars at all curing ages. The experimental results also indicated that DMA–MMA did not only change the rate of cement paste hydration, but also the microstructure of calcium–silicate–hydrate (C–S–H).
© 2007 Elsevier Ltd. All rights reserved.

Keywords: Retardation; Microstructure; Strength; Chemical admixture; Cement paste; Diblock copolymer

1. Introduction

In recent years, investigation and production of composite cements based on the partial replacement of Portland cement by waste materials have made considerable progress [1–4]. The replacement materials participate in the hydraulic reactions, contributing significantly to the composition and microstructure of the hydrated product. Among these materials, are industrial by-products, such as borogypsum from boric acid production plants, colemanite ore waste (CW), and tincal ore waste (TW) from enrichment process in boron plants. These materials contain significant amount of boron impurity, which has a positive contribution to the long-term strength development of the mortar [3]. However, the presence of boron in cement leads to a reduction in the early strength of the mortar and retards the cement setting. The setting time and early strength must be regulated by suitable activator to satisfy the demand of building engineering.

The accelerating water-reducing admixtures give greater strengths during the earlier hydration period and faster setting times, which allow the finishing operation to be carried out in a timely manner [5]. This product type is formulated using water-reducer ingredients (such as lignosulfonates and hydroxycarboxylic acid), and a high proportion of accelerators (calcium chloride or calcium formate). However, one of the limitations of the use of water-reducing admixtures containing calcium chloride in reinforced concrete is that when present in larger amounts, they promote corrosion of the reinforcement. Hence, there is a continuing attempt at finding an alternative additive to calcium chloride, one equally effective but without these limitations.

Our earlier studies showed that increasing replacement of Portland cement by TW resulted in a strength reduction of concrete and retarded setting time of the cement [3].

* Corresponding author. Tel.: +90 274 2652051; fax: +90 274 2652056.
E-mail address: aolgun@dumlupinar.edu.tr (A. Olgun).

0958-9465/$ - see front matter © 2007 Elsevier Ltd. All rights reserved.
doi:10.1016/j.cemconcomp.2007.05.002

Therefore, there is a need to find out a chemical, which will increase early strength of the mortar and not retard setting time of the cement. The aim of the present study was to determine the effect of the addition of DMA–MMA diblock copolymer on the setting characteristics of the cement paste and strength development of the mortar. After analysis of the morphology of hydrated cement phases, the content of calcium hydroxide was determined. The infrared spectra of DMA–MMA and cement paste were compared. Techniques for microstructural characterization, such as infrared spectroscopy, differential thermal analysis, thermogravimetric analysis and scanning electron microscopy, were also employed.

2. Experimental procedure

2.1. Raw materials

Raw materials were Portland cement clinker (PC), gypsum (G) from Denizli Cement Plant (Denizli, Turkey), and tincal ore waste from Eti-Boron Plant (Eskişehir, Kırka, Turkey). The chemical compositions of main raw materials are listed in Table 1. The hydrophilic–hydrophobic DMA–MMA [2-(dimethylamino) ethyl methacrylate]-[methyl methacrylate] diblock copolymer used in this study was synthesized by group transfer polymerization. The number of average molecular wight (M_n) and molecular weight distribution (PD) determined by gel-permeation chromatograph was 40,000 and 1.10, respectively. The DMA content of the DMA–MMA diblock copolymer was 92 mol% as determined by ^{1}H NMR spectroscopy. The details of the synthesis are reported elsewhere [6,7].

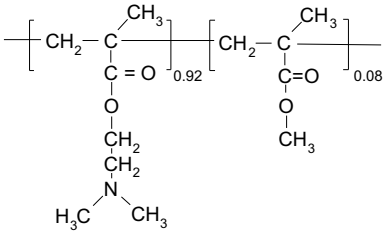

Table 1
Chemical characteristics of used material

	Chemical analysis (wt%)		
	Clinker	Tincal waste	Gypsum
SiO_2	21.22	10.95	0.94
Al_2O_3	4.28	0.91	0.54
Fe_2O_3	5.05	1.47	0.37
CaO	66.04	14.90	32.46
MgO	1.47	7.57	1.71
SO_3	1.20	0.43	42.56
Na_2O	0.22	12.00	0.47
K_2O	0.63	1.31	0.25
B_2O_3	–	9.70	–
Loss on ignition	0.16	39.06	20.78

2.2. Cement mixtures

Two series of mixtures noted as P(96%PC + 4%G) and T(93.3%PC + 3.7%G + 3%TW) were prepared according to TS-EN 197-1 [8]. The raw materials mixed in the required proportion were ground using a laboratory type grinding mill to a fineness of ≈27% mass residue on 32-μm-size mesh. Particle size analysis was carried out according to TS EN 196-6 [8]. The fineness of the cement was determined by Blaine specific surface area equipment.

2.3. Preparation of cement paste

The required water of standard consistency, setting time, and volume expansion were examined according to TS-EN 196-3 [8]. The mixing of cement pastes was carried out with the standard water of consistency as given in Table 2. Two reference pastes were prepared from the cements designated as P and T with deionized water only. DMA–MMA was added to the mixing water before mixing operation. The dosages of DMA–MMA were 0.1 and 0.5 mass% of the cement. The cement pastes were obtained using a mixer for 1 min at low speed (60 rpm) and 4 min at high speed (120 rpm). The paste was then poured into moulds creating 100 × 10 × 10 mm prisms. The samples were cured at 20 ± 2 °C and 90 ± 2% relative humidity. The samples were

Table 2
Water percent, setting time, and physical characteristics of cementitious mixes

Symbol	Cement mixes	Water (%)	Setting time (min)		Fineness (wt%)		Volume expansion (mm)			Density (kg/m^3)	Specific surface (m^2/kg)
			Initial	Final	+32 μ	90 μ	Cold	Hold	Total		
P		25	190	240	27	1	1	1	2	3.15	352.7
P_1	P + 0.1%DMA–MMA	25.5	200	250			0	0	0		
P_2	P + 0.2%DMA–MMA	26.0	210	260			0	0	0		
P_3	P + 0.3%DMA–MMA	26.5	220	270			0	0	0		
P_4	P + 0.4%DMA–MMA	27.0	230	270			0	0	0		
P_5	P + 0.5%DMA–MMA	28.0	240	270			0	0	0		
T		26	300	380	27.2	1.0	1	1	2	3.13	352.0
T_1	T + 0.1%DMA–MMA	26.5	310	390			0	0	0		
T_2	T + 0.2%DMA–MMA	27.0	320	400			0	0	0		
T_3	T + 0.3%DMA–MMA	27.5	330	400			0	0	0		
T_4	T + 0.4%DMA–MMA	28.0	340	400			0	0	0		
T_5	T + 0.5%DMA–MMA	28.2	350	400			0	0	0		

then demolded and placed in deionized water. The cement paste specimens were cured for 2, 7, and 28 days, and then they were taken out of the water. The hydration process was stopped by grinding the hydrated samples with acetone and by washing the residue several times with more acetone. The samples were dried at 65 °C.

2.4. Compressive strength test

The specimen preparation for strength tests was performed at room temperature. Mortar specimens were produced by mixing one part of the cement with three parts of sand, using two different water-to-cement ratios (w/c) of 0.50 and 0.42. DMA–MMA diblock copolymer was added to mixing water during the mixing operation. The dosages of DMA–MMA diblock copolymer were 0.1, 0.2, 0.3, 0.4, and 0.5 mass% of cement. The cement–water mixtures were stirred at low speed for 30 s, and then, with the addition of sand, the mixtures were stirred for 4 min. The mortars prepared were cast into $40 \times 40 \times 160$ mm moulds for strength tests. After 24 h of curing at 20 °C, the samples were demolded, and then immediately immersed in a water-curing tank. The temperature of the water was maintained at 20 ± 1 °C during the curing period. The compressive strength test was carried out at the ages of 2, 7, and 28 days according to TS EN 196-1 [8]. The strength value was the average of three specimens.

3. Characterization

3.1. Scanning electron microscopy

For scanning electron microscopy (SEM) studies, selected cement paste samples cured for 28 days were used. A cement prism was cut into cubes of approximately 10 mm square, one side of which was ground flat. The hydrated samples were soaked in acetone to stop hydration reactions. After drying the sample of specimens were coated with gold, and then the SEM images of samples were obtained using a JEOL JXA 840A scanning electron microscope.

3.2. X-ray diffraction

A piece of hydrated cement paste prism was taken and was ground to a fine powder of <63 μm. A Rikagu Miniflex X-ray diffractometer using mono-chromatic CuKα radiation operating at a voltage of 30 kV and current of 15 mA was used. A scanning speed of 2°2θ/min and a step size of 0.02° were used to examine the samples in the range of 5–75°2θ.

3.3. Infrared spectroscopic test

The FT-IR spectra of both the 28-day hydrated neat cement and DMA–MMA diblock copolymer modified cement pastes were recorded on a Bruker Vertex 70 FT-IR spectrometer equipped with the harric MVP2-unit in the range of 4000–400 cm^{-1} region.

3.4. Differential thermal analysis

DTA and thermo gravimetric analysis (TG/DTA) of the selected 28-day hydrated sample were obtained using a Shimadzu, DTG-60H Simultaneous DTA-TGA apparatus. The samples were heated from 35 to 1100 °C at a constant rate of 10 °C/min in nitrogen gas dynamic atmosphere (100 cm^3/min). All the weight loss data are expressed as a

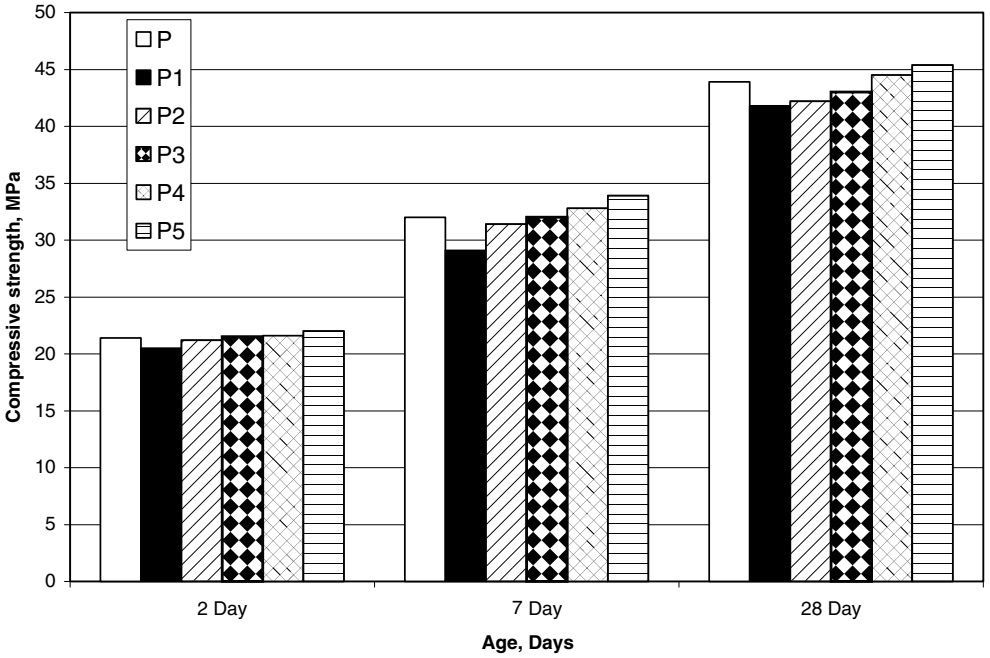

Fig. 1. Effects of DMA–MMA diblock copolymer on the compressive strength of the PC mortar (water to cement ratio, 0.50).

function of the ignited weight of the sample as suggested by Taylor [9]. The amount of portlandite CH (%) was obtained directly from TG curves by Eq. (1):

$$CH(\%) = WL_{CH(\%)} \frac{MW_{CH}}{MW_H} \quad (1)$$

where $WL_{CH(\%)}$ corresponds to the weight loss, in percent, occurring during CH hydration, and MW_{CH} and MW_H are the molecular weights of portlandite and water, respectively.

4. Results and discussion

4.1. Setting characteristics and volume expansion

The initial and final setting time of the Portland cement and TW cement are given in Table 2. The initial and final

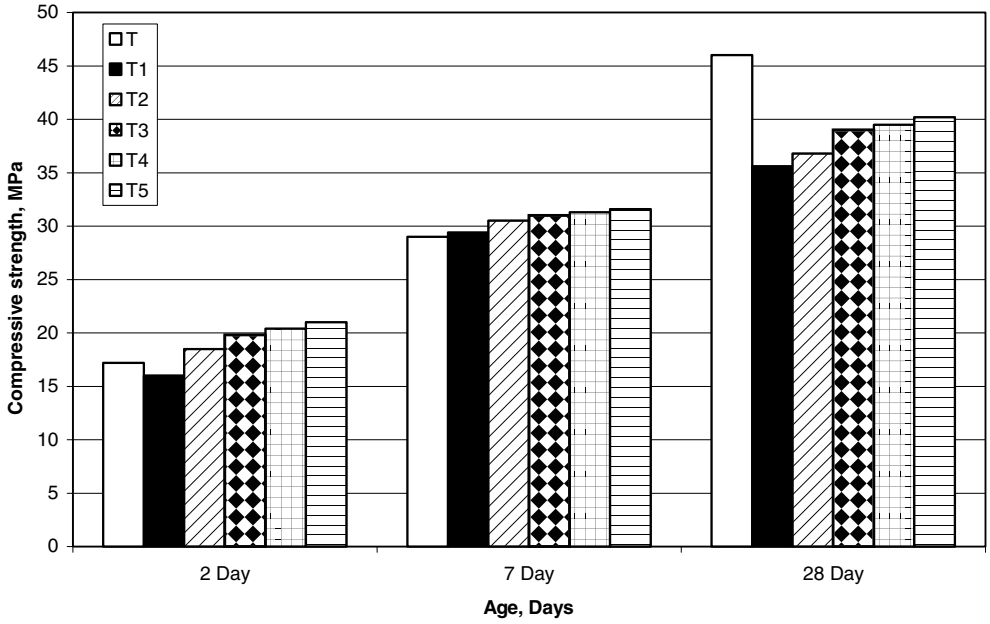

Fig. 2. Effects of DMA–MMA diblock copolymer on the compressive strength of the TW mortar (water to cement ratio, 0.50).

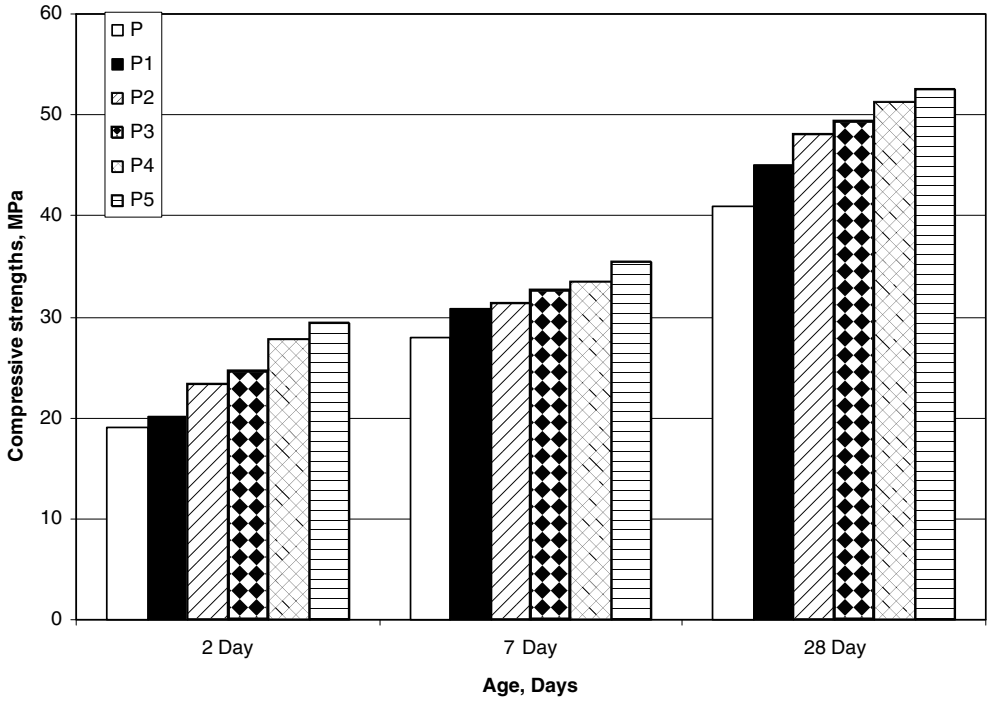

Fig. 3. Effects of DMA–MMA diblock copolymer on the compressive strength of the PC mortar (water to cement ratio, 0.42).

setting times of the neat cement and cement containing boron were found to be 190 and 240 min, and 300 and 380 min, respectively. Many workers have reported that the presence of boron in the cement retards the cement setting [1,3]. J. Bensted et al. observed this retardation and attributed it to a coating effect and the inhibition of calcium hydroxide nucleation [10]. Apagyi and Csetenyi also noted that the boron in the cement increased portlandite solubility [11].

Table 2 shows that the initial setting times of cements are prolonged by the addition of DMA–MMA diblock copolymer. With the increase of the amount of DMA–MMA diblock copolymer, the initial setting times of the both cement and cement containing boron are gradually prolonged. Similarly, the inclusion of DMA–MMA diblock copolymer into the cement up to 0.3% (weight of cement) extends the final setting time of the both cements in the same extends. It is interesting that DMA–MMA diblock copolymer slightly increases the final setting time of the PC and TW cement, and the retarding ability diminish with the increase of the polymer content. The present study is not concerned to reveal the nature of the mechanism of retardation of DMA–MMA diblock copolymer. However, many investigators have concluded that the

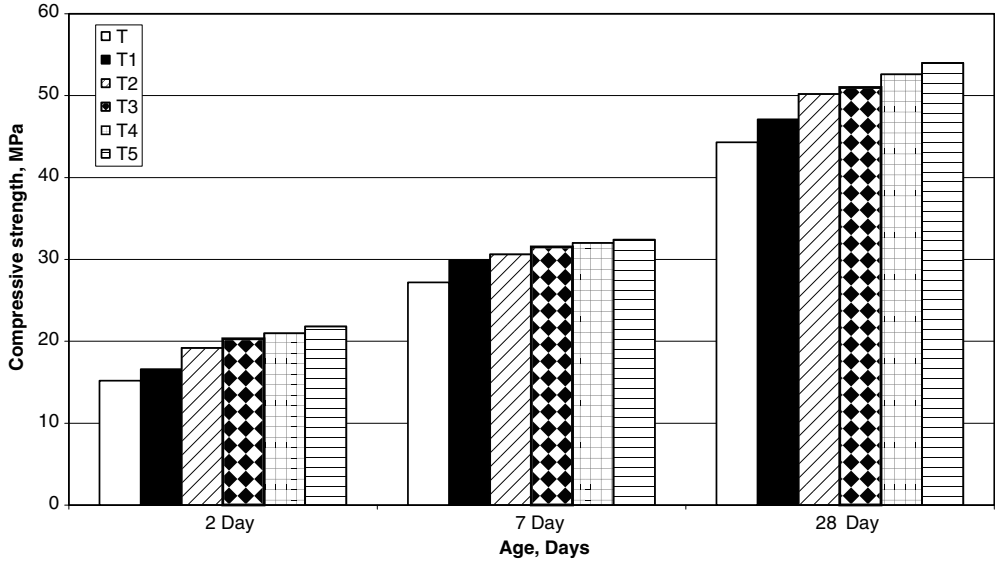

Fig. 4. Effects of DMA–MMA diblock copolymer on the compressive strength of the TW mortar (water to cement ratio, 0.42).

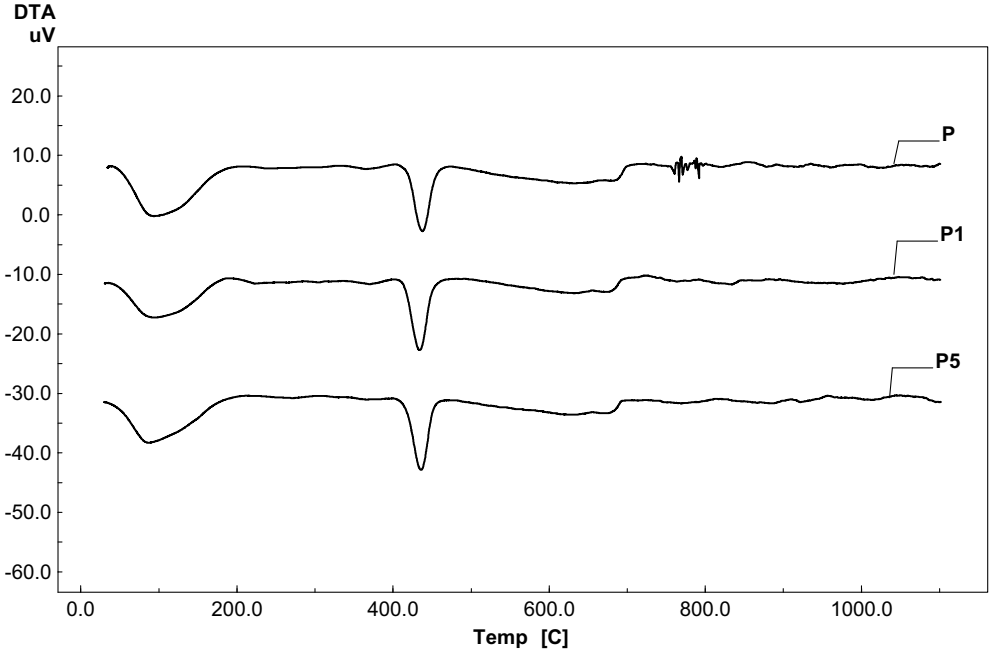

Fig. 5. DTA/TG of the hydrated Portland cement pastes (with and without DMA–MMA diblock copolymer).

retarding action of the admixture is, in most cases, due to its effect on C_3S hydration and adsorption of the admixture on the surface of the cement particles [12,13]. It seems that the retardation process in the presence of DMA–MMA diblock copolymer is due to its tendency to decrease the surfaces areas available for the hydration of C_3S, and C_3A particles.

The effects of diblock copolymer on the volume expansion of cement paste are given in Table 2. The results indicate that DMA–MMA diblock copolymer slightly decreases expansion of cement paste compared to control cement paste containing no polymer. In polymer-modified systems, the possible factor behind the reduction in volume may be attributed to the

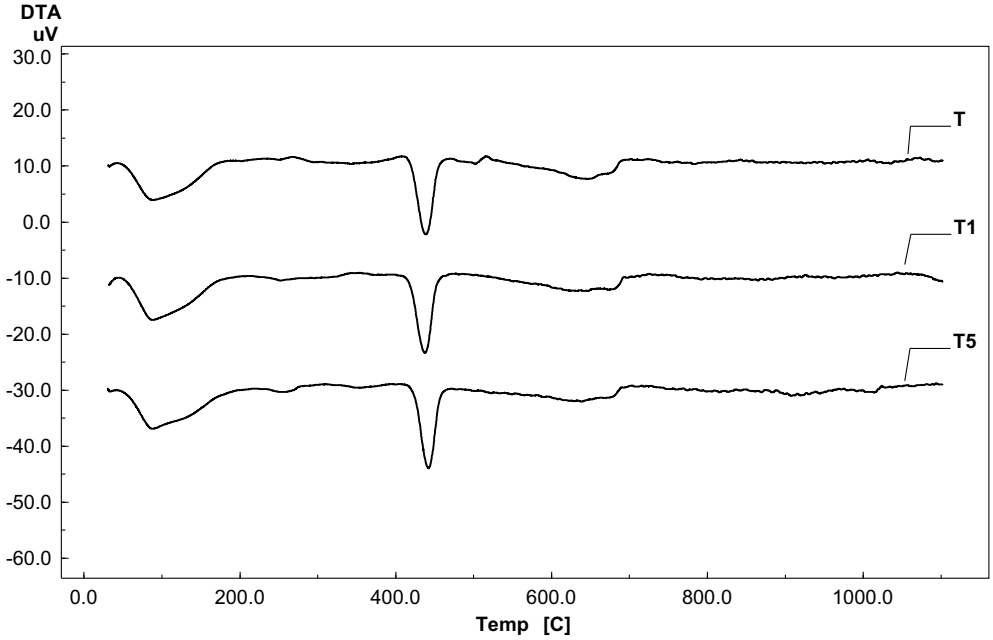

Fig. 6. DTA/TG of the hydrated TW cement pastes (with and without DMA–MMA diblock copolymer).

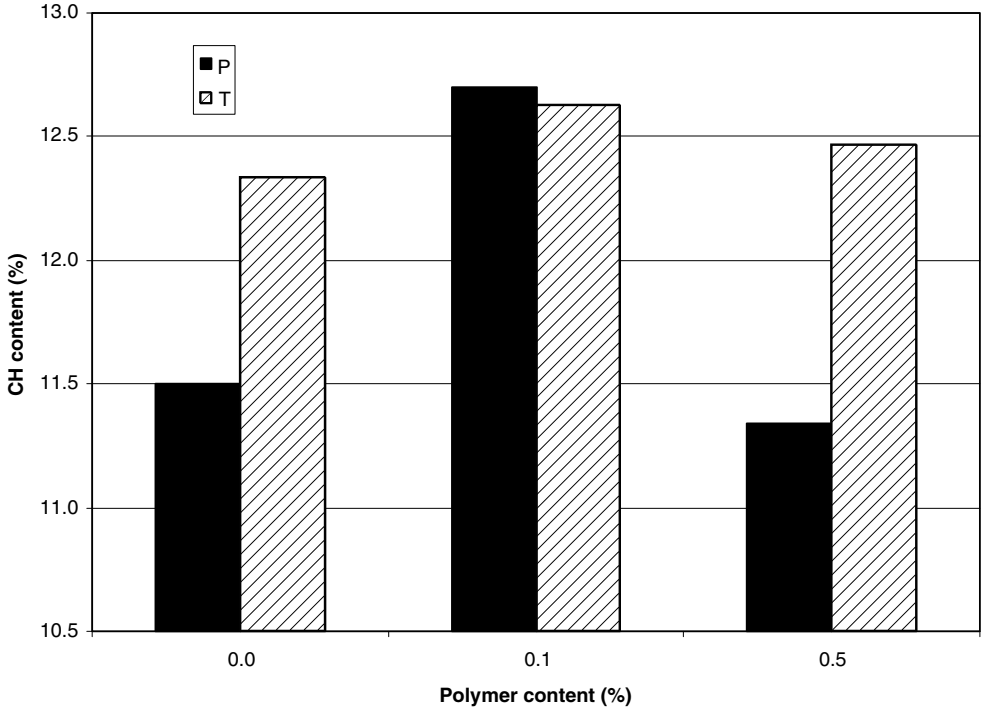

Fig. 7. Effect of DMA–MMA diblock copolymer content on the calcium hydroxide content (CH) of cement pastes.

attractive forces produced between polymer and hydrated cementitious particles.

4.2. Effect of DMA–MMA diblock copolymer on the strength development of mortar

The effects of DMA–MMA diblock copolymer on the strength development of PC and TW mortars ($w/c = 0.5$) are shown in Figs. 1 and 2. At 2 days of curing age, the compressive strength of the PC mortar and TW mortar without DMA–MMA diblock copolymer were observed as 19.0 and 15.2 MPa, respectively. The strength of the TW mortar considerably increased with the addition of the polymer beyond 0.1%, while the strength of the PC mortar slightly increased (Figs. 1 and 2). As curing time expanded to 7 days, the compressive strength of the DMA–MMA diblock copolymer activated TW mortars was higher than that of TW mortar containing no polymer, and the strength increased gradually with the increase of polymer content. The effect of polymer on strength of PC mortar showed similar trend as 2 days curing age. At 28 days, the compressive strength of the polymer activated TW mortar was lower than that of TW mortar without DMA–MMA diblock copolymer. This observation shows that incorporation of DMA–MMA diblock copolymer in mortar clearly influences the hydration process. The

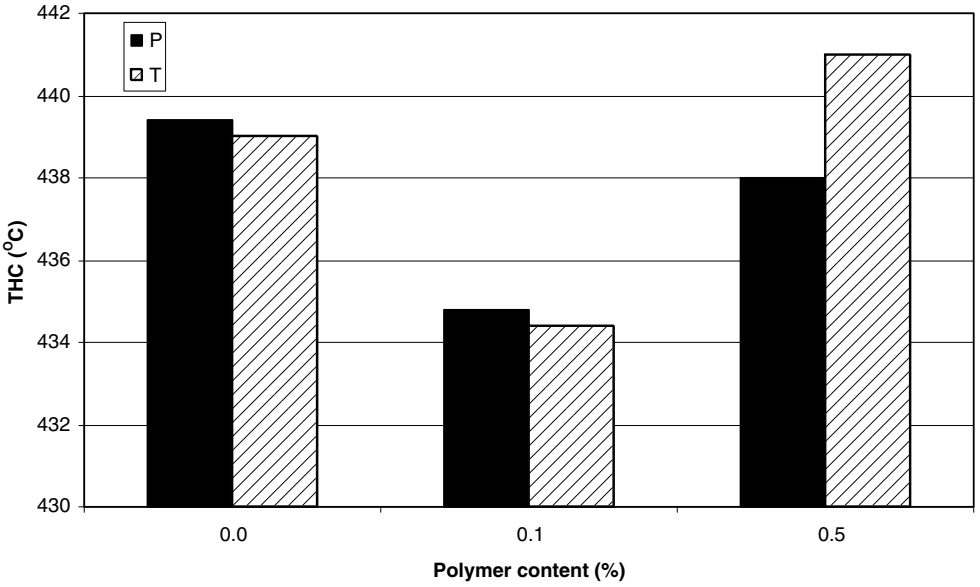

Fig. 8. Effect of DMA–MMA diblock copolymer content on dehydration temperature (TCH) of cement pastes.

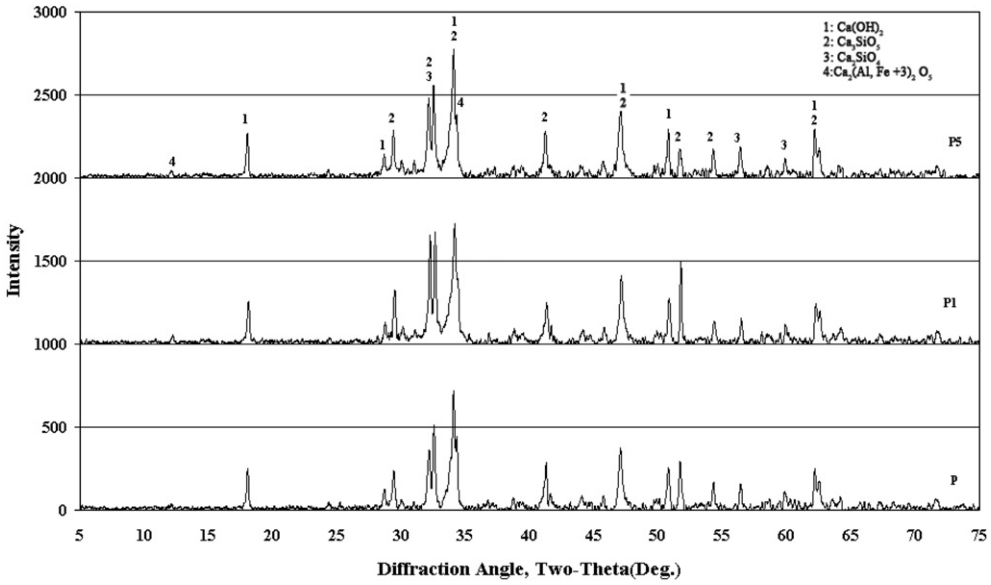

Fig. 9. XRD patterns of PC cement cured for 2 days (with and without DMA–MMA).

possible mechanism, which may lead to decreased strength in DMA–MMA diblock copolymer activated TW specimens, may be related to the fact that the presences of boron in cement affects the solubility of portlandite that alters the degree of the attractive forces produced between polymers and hydrated cementitious particles.

The effect of DMA–MMA diblock copolymer on the compressive strength of PC and TW mortars ($w/c = 0.42$) cured up to 28 days is given in Figs. 3 and 4. Apparently, the trend in Fig. 3 is similar to that in Fig. 4. The compressive strength of the DMA–MMA diblock copolymer modified mortars was higher than that of the mortars without DMA–MMA diblock copolymer. The strength values increased with the increasing DMA–MMA diblock copolymer content. This observation shows that compressive strength of the mortars can be improved at all curing ages by the addition of DMA–MMA diblock copolymer with a reduction water–cement ratio.

4.3. DTA analysis

Differential thermal analysis and TGA were used to study the effects of DMA–MMA diblock copolymer on the hydration of different cement phases. Three major endothermic reactions were occurred during the heating of the cement pastes hydrated for 28 days. As Bensted

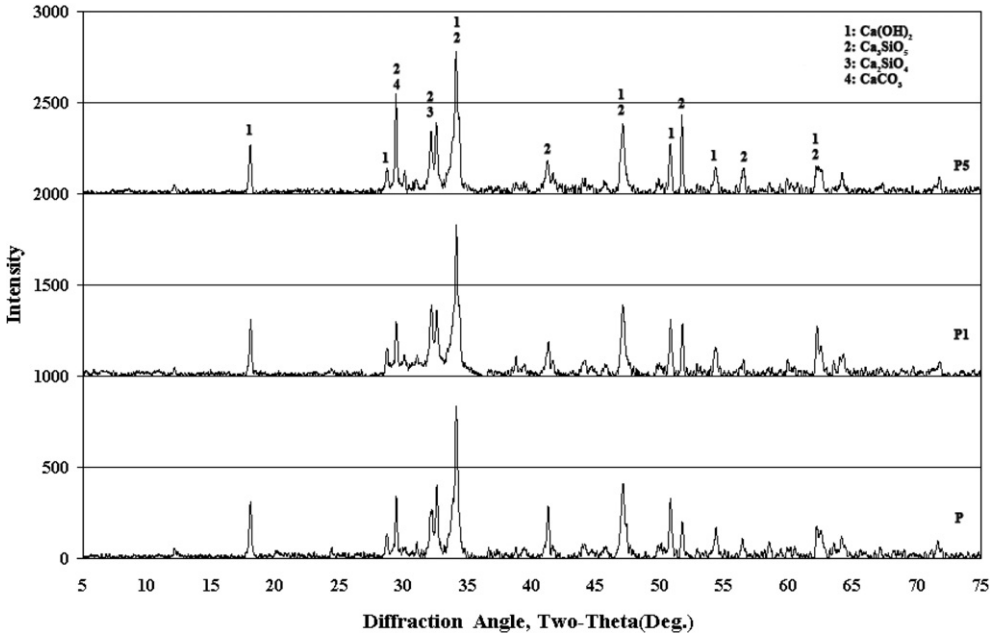

Fig. 10. XRD patterns of PC cement cured for 7 days (with and without DMA–MMA).

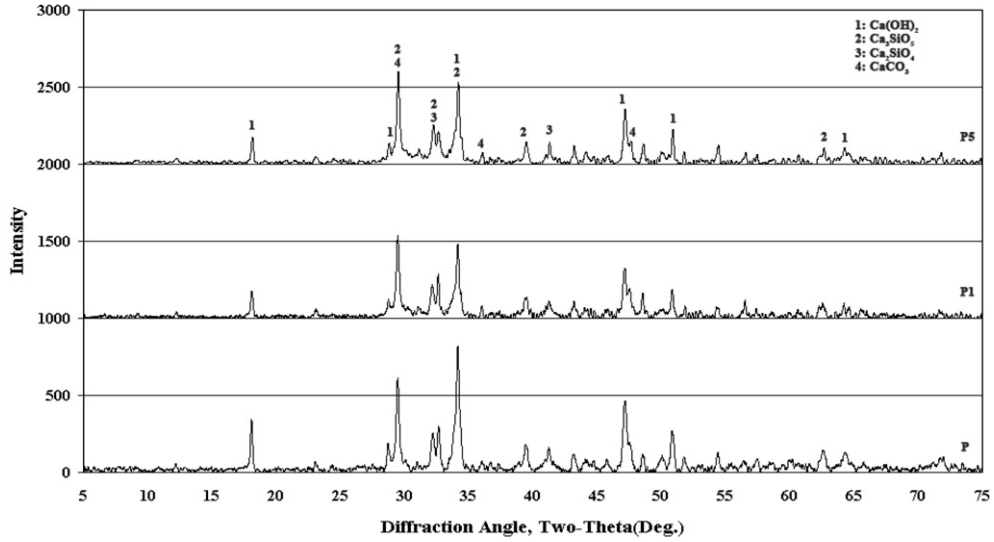

Fig. 11. XRD patterns of PC cement cured for 28 days (with and without DMA–MMA).

and Varma [14], and Odler and Abdul-Maula [15] suggested, the decomposition peaks of CSH (at 120 °C) and ettringite (at 145 °C) overlap beyond 4 h of hydration. Therefore, it is possible to assign the first peaks to CSH hydration and ettringite decomposition (Figs. 5 and 6). An endothermic peak at about 410–460 °C corresponds to the decomposition of calcium hydroxide to calcium oxide and water. An endothermic peak at about 650 °C is related to the decomposition of carbonate phases.

As shown in Figs. 5 and 6, DMA–MMA diblock copolymer influences the DTA curves of PC and TW cement pastes. Cement pastes with 0.1% DMA–MMA show a slight decrease in the dehydration temperature of CH. When more DMA–MMA diblock copolymer is present (0.5%), dehydration temperature of CH increases for both cement pastes (Fig. 8). Fig. 7 shows that DMA–MMA diblock copolymer (0.5%) considerably increases the quantity of CH phases in the pastes. It is not that the amount of CH in PC cement paste without DMA–MMA diblock copolymer is lower than that of TW cement paste. This result indicates that the presence of boron impurity in the cement paste has remarkable effects on the development of CH in the cement. The addition of a higher level of DMA–MMA diblock copolymer limited the development

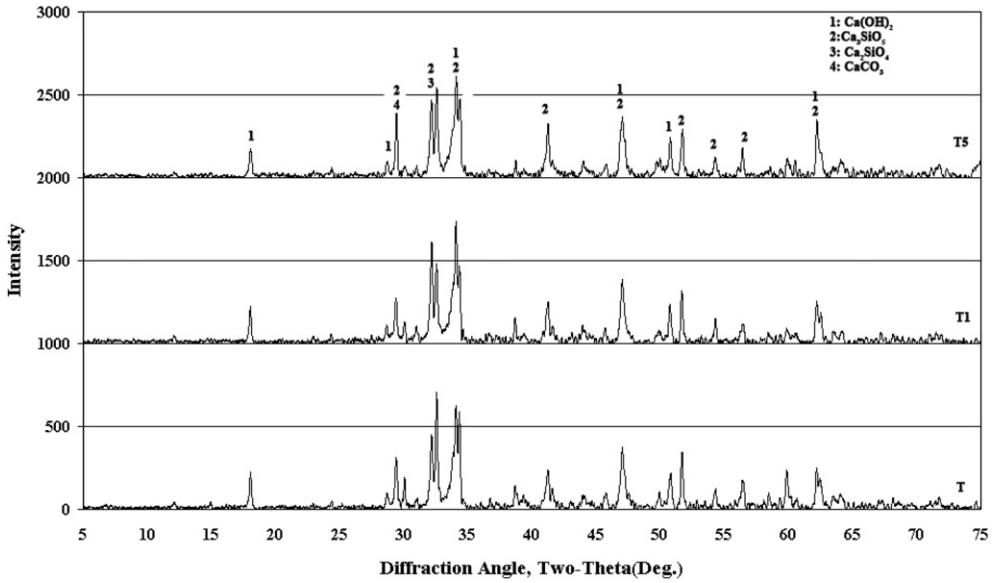

Fig. 12. XRD patterns of TW cement cured for 2 days (with and without DMA–MMA).

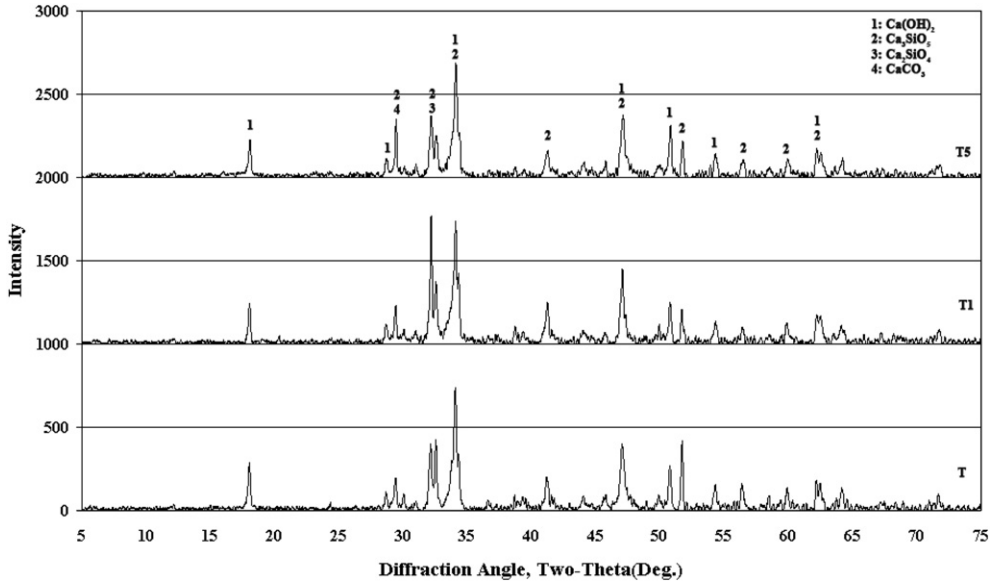

Fig. 13. XRD patterns of TW cement cured for 7 days (with and without DMA–MMA).

of CH as demonstrated by mix P5, where the extent of CH formation was significantly lower than for other mixtures.

4.4. X-ray diffraction

The development in time of the two cement systems (with and without polymer), as indicated by XRD, is shown in Figs. 9–14. They show the X-ray patterns obtained after 2, 7, and 28 days of curing. The XRD patterns indicating the hydration of the neat cement and polymer activated cement are shown in Fig. 9. The expected crystalline hydration products are evident. Calcium hydroxide was formed with appreciable amounts in two days, and remained a good crystalline reaction product throughout the period of investigation. The amount of $Ca(OH)_2$ increased with increasing DMA–MMA diblock copolymer content. Calcium carbonate was formed after 7 days of curing age (Fig. 10). The relative amount of calcium carbonate in these XRD patterns can be attributed to the carbonation of $Ca(OH)_2$. In the case of C_3S phases, the peaks of maximum intensity overlap with those of C_2S, which makes its evolution difficult to determine. Therefore, their trend can be interpreted jointly. The amount of these phases decreased with increasing time and DMA–MMA diblock copolymer content. There is a marked difference in the XRD patterns of the cement cured for 7 days. Calcium hydroxide was formed in greater amounts in control system, and the amount decreased with increasing DMA–MMA diblock copolymer content.

The X-ray traces for the TW cement paste are shown in Figs. 12–14. The phases identified were: calcium hydroxide, C_3S, C_2S, and calcium carbonate. The amount of the

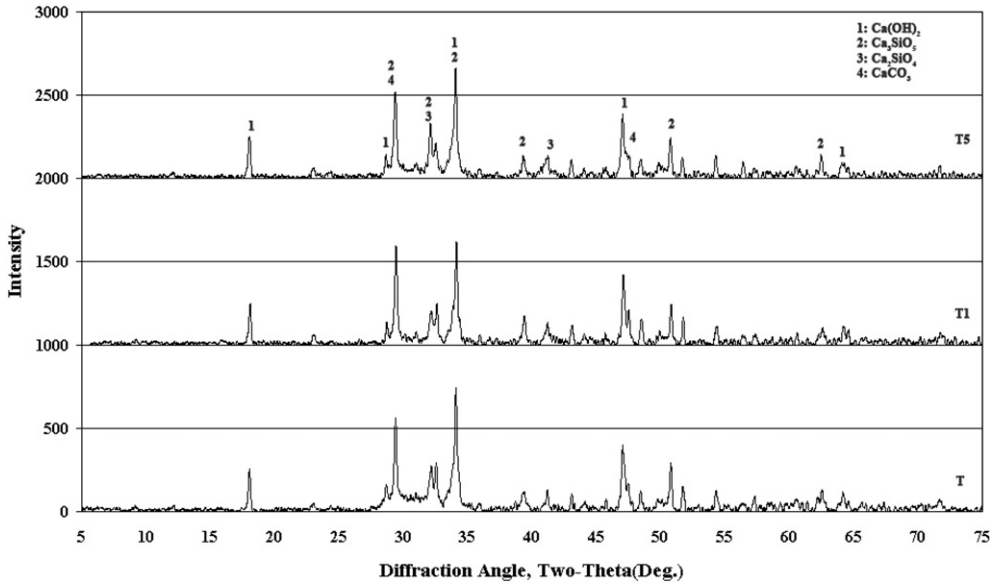

Fig. 14. XRD patterns of TW cement cured for 28 days (with and without DMA–MMA).

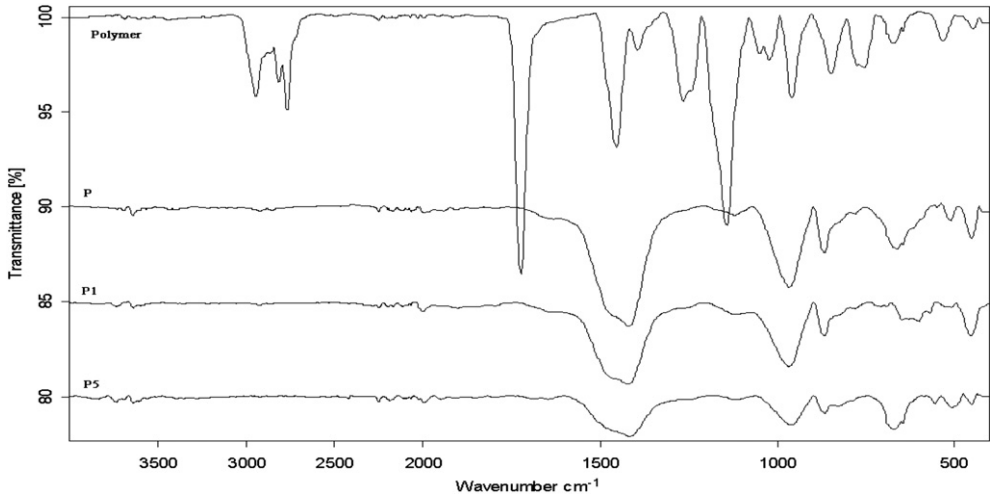

Fig. 15. Fourier-transform infrared spectrum of Portland cement pastes (with and without DMA–MMA diblock copolymer).

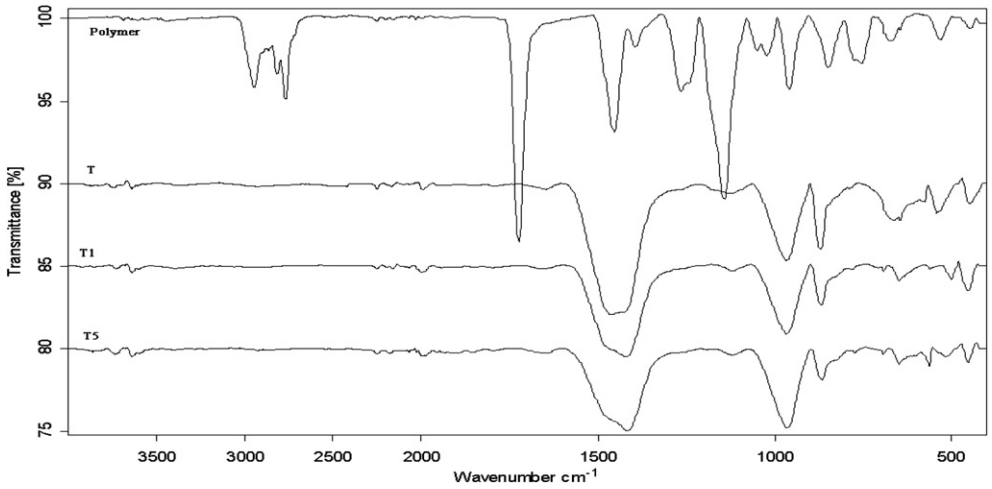

Fig. 16. Fourier-transform infrared spectrum of TW cement pastes (with and without DMA–MMA diblock copolymer).

calcium hydroxide present in cement increase slightly during the curing ages. The peak of calcium carbonate appeared at 7 days of hydrated cement (Fig. 13) and the intensity of it increased with increasing curing time (Fig. 14).

The results show some qualitative differences in the hydration rate of the two different cement systems due to the incorporation of DMA–MMA diblock copolymer. With regards to the formation of calcium carbonate, it can be observed that the incorporation of DMA–MMA diblock copolymer leads to a fast increase in calcium carbonate content in PC cement. The rate of the formation of calcium hydroxide in PC cement is also higher between 2 and 7 days, indicating a faster growth of the C–S–H phase.

4.5. IR spectroscopy study

The IR spectra of 28-day hydrated cements (with and without admixture) are shown in Figs. 15 and 16. The spectrum of Portland cement without DMA–MMA diblock copolymer shows band at 3639, 1419, 1121, 966, 868 661, 511, and 451 cm^{-1}. The band observed at about 3639 cm^{-1} is due to the OH band from $Ca(OH)_2$. The bands observed at 1419 cm^{-1} show the presence of calcium carbonate in the hydrated cement past, and the peak intensity decreases with increasing DMA–MMA diblock copolymer content for both cement pastes. The band observed at 868 cm^{-1} can be attributed to the presence of anhydrated dicalcium silicate (C_2S) in the pastes. Regardless of cement type, the intensity of the band gradually decreases with increasing DMA–MMA diblock copolymer content. This result indicates that the presence of DMA–MMA in the cement paste has positive contribution to the hydration rate of C_2S.

Previous studies have shown that the strongest Si–O stretching (v_3) bands appeared at 925 cm^{-1}, Si–O bending (v_4) vibration at 524 cm^{-1}, and Si–O bending (v_5) vibra-

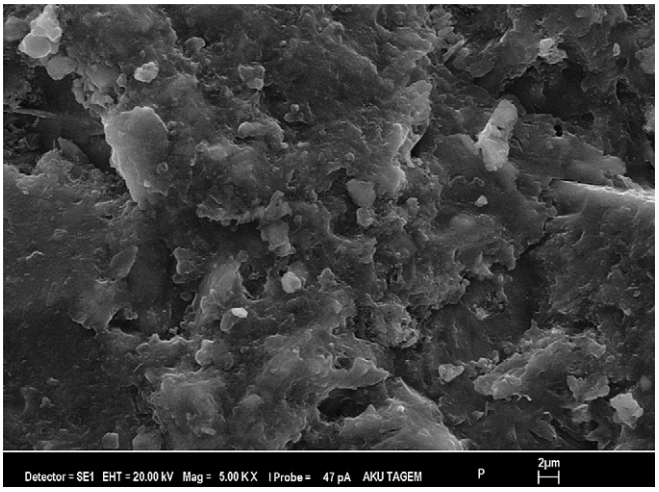

Fig. 17. SEM micrographs of fracture surface of cement paste after 28 days of hydration (without DMA–MMA diblock copolymer).

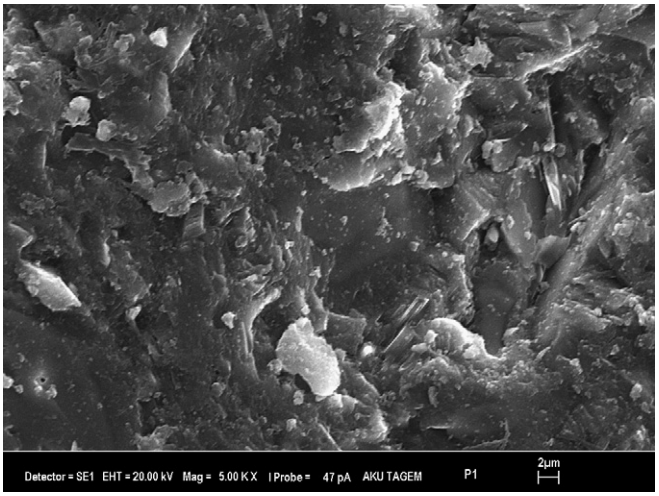

Fig. 18. SEM micrographs of fracture surface of cement paster after 28 days of hydration (with 0.1% DMA–MMA diblock copolymer).

tions at 460 cm^{-1} in dry cement [16]. In our study, the shifting of Si–O asymmetric stretching (v_3) vibration to higher wave numbers (961–967 cm^{-1}) indicates the polymerization of silicate units SiO_4^{4-} with the formation of the CSH phase [17]. Relative intensity of the Si–O stretching (v_3), Si–O bending (v_4) vibration at 524 cm^{-1}, and Si–O bending (v_5) vibration bands also undergoes significant changes as a result of polymerization of the SiO_4^{4-} in PC and TW cement paste. The intensity of Si–O stretching (v_3) vibration bands for PC cement paste gradually decreased with the increasing DMA–MMA diblock copolymer content (Fig. 15).

4.6. SEM observation of microstructure

Scanning electron micrographs of selected cement paste (with and without DMA–MMA diblock copolymer) hydrated for 28 days are presented in Figs. 17–22. The microstructure of the PC cement paste without polymer shown in Fig. 17 indicates a comparatively dense microstructure, typical of a sound Portland cement paste. A very large $Ca(OH)_2$(CH) crystal and a porous composite mass of calcium silicate hydrate (CSH) are also observed. Fig. 18 shows that the morphology of crystallite size of CH phase is significantly affected by polymer. The crystallites are smaller and thinner with the presence of polymer than with the PC paste containing no admixture. In the PC cement containing 0.5% DMA–MMA diblock copolymer, the CH has been significantly converted the hydration products, and a very dense structure of CSH has been formed (Fig. 19). A polymeric film partially covering the hydrated phases was also observed.

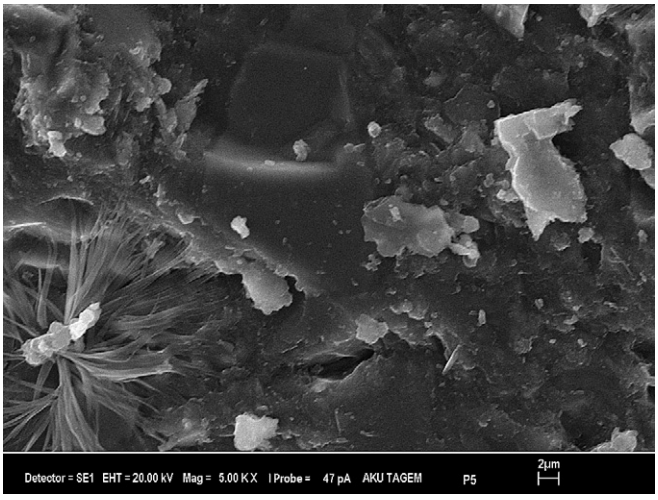

Fig. 19. SEM micrographs of fracture surface of cement paste after 28 days of hydration (with 0.5% DMA–MMA diblock copolymer).

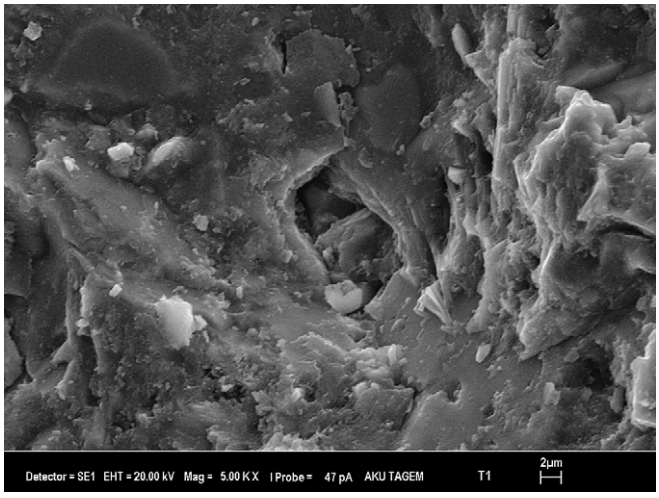

Fig. 21. SEM micrographs of fracture surface of cement paste containing tincal ore waste after 28 days of hydration (with 0.1% DMA–MMA diblock copolymer).

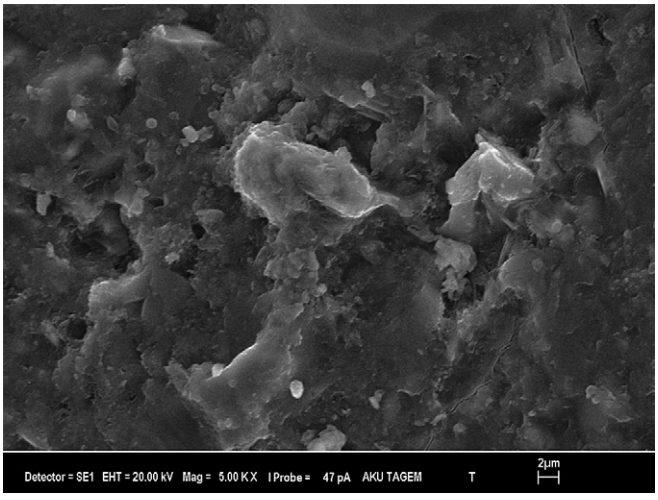

Fig. 20. SEM micrographs of fracture surface of cement paste containing tincal ore waste after 28 days of hydration (without DMA–MMA diblock copolymer).

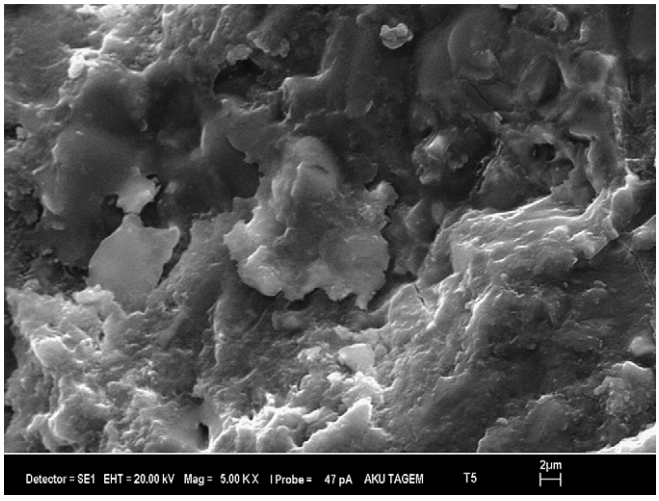

Fig. 22. SEM micrographs of fracture surface of cement paste containing tincal ore waste after 28 days of hydration (with 0.5% DMA–MMA diblock copolymer).

The micrograph of TW cement paste is shown in Fig. 20 at the same magnification with Fig. 17 to allow direct comparison. The microstructure is notably different from that developed in the PC cement paste, where very dense structures of CSH were observed. The morphology of the TW cement paste with polymer (0.1%) was similar to that of the PC cement containing same amount of polymer, but the cement hydration products seemed to be localized in TW cement paste (Fig. 21). Compared to PC cement paste with 0.5% polymer (Fig. 22), TW cement paste has a denser deposit of CH encapsulating CSH dense structure. This may be attributed to the effect of boron impurity on the hydration rate of cement.

5. Conclusions

In this study, the effect of DMA–MMA diblock copolymer on the properties of ordinary Portland cement and cement containing boron has been investigated. It is worth mentioning that this is a preliminary study on the use of DMA–MMA diblock copolymer as a chemical admixture. Moreover, based on the experimental result, the following conclusions are confirmed:

1. The replacement of Portland cement clinker by tincal ore waste decreases the compressive strength of the mortar at early ages, but the strengths of the mortar are comparable to that of the PC mortar at 28 days of curing age.
2. The addition of DMA–MMA diblock copolymer up to 0.3% (weight of cement) to the mortar containing PC cement slightly decreases the compressive strength of the samples at all curing ages. However, the use of DMA–MMA diblock copolymer in PC cement significantly increases 7-day strength of the mortars, and decreases 28-days strength.
3. DMA–MMA diblock copolymer allows a significant reduction in the water to cement ratio, which accelerates the strength development of PC and TW mortars at all curing ages.
4. The addition of up to 0.3% (weight of cement) DMA–MMA diblock copolymer to the PC and TW cement pastes retard the initial setting time and have no noticeable effect on the final setting time of the cement.
5. The hydration products formed in the two systems studied were corresponds to the effected products, although they differed in magnitude. Calcium hydroxide is formed initially in all systems, remaining as a good crystalline reaction product throughout the period of investigation.
6. The DMA–MMA diblock copolymer modified cement pastes shows a dense microstructure compared to that of cement pastes without activator.

Acknowledgements

The authors thank Denizli Cement Plant (Denizli, Turkey) for providing facilities of mechanical testing of materials. V. Bütün thanks Turkish Academy of Science for an encouragement award for science scholarship. We also wish to thank Mrs. Birgül Muş for many helpful discussions.

References

[1] Targan Ş, Olgun A, Erdoğan Y, Sevinç V. Effects of supplementary cementing materials on the properties of cement and concrete. Cement Concrete Res 2002;32:1551–8.
[2] Yan P, Yang W. The cementitious binder derived with flurogypsum and low quality of fly ash. Cement Concrete Res 2000;30:275–80.
[3] Kula I, Olgun A, Sevinc V, Erdogan Y. An Investigation on the use of tincal ore waste, fly ash and coal bottom ash as Portland cement replacement materials. Cement Concrete Res 2002;32:227–32.
[4] Hill J, Sharp JH. The mineralogy and microstructure of three composite cement with high replacement levels. Cement Concrete Comp 2002;24:191–9.
[5] Rixom MR. Chemical admixtures for concrete. London: Spon; 1999.
[6] Baines FL, Billingham NC, Armes SP. Synthesis and solution properties of water-soluble hydrophilic–hydrophobic block copolymers. Macromolecules 1996;29(10):3416–20.
[7] Bütün V, Armes SP, Billingham NC. Synthesis and aqueous solution properties of near-monodisperse tertiary amine methacrylate homopolymers and diblock copolymers. Polymer 2001;42:5993–6008.
[8] TS EN-196-1, TS EN-196-3, TS EN-196-6, TS-EN 197-1, Turkish National Standards. Ankara, Turkey: TSE Turkish Standard Institute.
[9] Taylor HFW. Studies on the chemistry and microstructure of cement pastes. Pro Br Ceram Soc 1984;35:65–82.
[10] Bensted JB, Callaghan IC, Lepre A. Comparative study the efficiency of various borate compounds as set-retarders of class G oilwell cement. Cement Concrete Res 1991;21:663–8.
[11] Apagyi Z, Csetenyi LJ. Phase equilibrium study in the $CaO–K_2O–B_2O_3–H_2O$ system at 25 °C. Cement Concrete Res 2001;31:1087–91.
[12] Yilmaz VT, Glasser FP. Influence of sulphonated melamine formaldehyde superplasticizer in cement. Adv Cement Res 1989;2:111–9.
[13] Barnes P. Structure and performance of cement. USA: Routledge; 2001.
[14] Bensted J, Varma SP. Some applications of infrared and Raman spectroscopy in cement chemistry: Part 3. Hydration of Portland cement and its constituents. Chem Technol 1974(September/October):440–50.
[15] Odler I, Abdul-Maula S. Possibilities of quantitative determination of Aft-(ettringite) and Afm (monodulphate) phases in hydrated cement pastes. Cement Concrete Res 1984;14:133–41.
[16] Perraki Th, Kakali G, Kontoleon F. The effect of natural zeolites on the early hydration of portland cement. Micropor Mesopor Meter 2003;61:205–12.
[17] Mollah MYA, Yu Wenhong, Schennach Robert, Cocke David L. A fourier transform infrared spectroscopic investigation of the early hydration of Portland cement and the influence of sodium lignosulfonate. Cement Concrete Res 2000;30:267–73.